A MODEL FOR STRAIN-TEMPERATURE LOOPS IN SHAPE MEMORY ALLOY ACTUATORS

Maria Marony S. F. Nascimento
José Sérgio da Rocha Neto
Antonio Marcus Nogueira de Lima
Departamento de Engenharia Elétrica
Universidade Federal de Campina Grande
Cep: 58109-970
Campina Grande – PB Brazil
Luis A. L. de Almeida
Departamento de Engenharia Elétrica
Universidade Federal da Bahia
Salvador – BA Brazil
Carlos José de Araújo
Departamento de Engenharia Mecânica
Universidade Federal de Campina Grande
Cep: 58109-970
Campina Grande – PB Brazil
Carlos@dem.ufpb.br

Abstract: *In this paper, a hysteresis model, originally developed for magnetic hysteresis and adapted to thermal hysteresis in vanadium dioxide (VO_2) thin films, is proposed to describe the hysteresis in the ε-T characteristics of a SMA actuator. In order to determine the strain (ε) - Temperature (T) behavior of a Ti-Ni SMA wire actuator (78mm in length and 150μm in diameter) an experimental set-up was implemented. The SMA wire is loaded with a weight providing a constant uniaxial tensile stress and is heated electrically. In the absence of an accurated and reliable technique for measurement of the SMA wire temperature, such temperature is estimated from the electrical current using the static thermal equilibrium equation for the steady-state. External room temperature disturbances are greatly reduced by embedding the wire in a heat-insulating medium. The control of the heating electrical current through the wire and measurement of the steady-state wire deformation with an LVDT displacement sensor having a resolution of 5μm, was done using GPIB compatible instruments. The results of these measurements, for ε-T major loops and first order descending curves, are presented together with the data calculated with the proposed model. Model simulations have shown good agreement with the experimental data.*

Keywords: *Shape memory alloy actuators, hysteresis models, smart materials.*

1. Introduction

Shape memory alloys (SMA) have been considered one of the more interesting smart material systems, with a great potential for applications in some modern active structures, mainly as electrical or thermal actuator (Srinivasan and McFarland, 2001). Previously strained SMA actuator recover its original shape when heated above a critical temperature. In the case of SMA wire actuators under uniaxial tensile mechanical load, this shape recovery corresponds to a contraction and the actuator provides a useful external mechanical work. However, the thermoelastic martensitic transformation at the origin of this shape memory effect (SME) is characterized by four transformation temperatures (M_s, M_f, A_s e A_f, typically in raising order) describing a hysteresis loop between two crystalline structures (Otsuka and Wayman, 1998). Then, the trajectory of the actuator is nonlinear and accompanied by a hysteresis. Thus, the analysis, design and optimization of a SMA actuator are critically dependent on the availability of a strain (ε) – temperature (T) hysteresis model that can mathematically describe this characteristic including both major and minor loops. Ortin and Delaey (2002) present an overview of hysteresis phenomena in the martensitic transformation, and their relevance in the thermomechanical behaviour of shape-memory alloys. A great number of constitutive models have been based on phenomenological continuum mechanics and plasticity (Helm and Haupt, 2003; Aurichio and Lubliner, 1997; Aurichio *et al.*, 1997; Aurichio and Sacco, 1997) and many others are based on a kinetic law governing the phase transformation behavior (Tanaka and Nagaki, 1982; Tanaka, 1986; Liang and Rogers, 1990; Brinson, 1993; Boyd and Lagoudas, 1994). The `former` models are mathematically complex and generally multidimensional while the later are of easy implementation and have been successfully applied for the analysis and design of some SMA active structures. Comparisons of SMA constitutive models with assumed transformation kinematics has demonstrated differences and a more realistic performance of the Brinson model (Paiva and Savi, 1999). For control purposes, Gorbet (1997) and Majima *et al.* (2001) proposed a model for phase transformation based on modification of the Preisach model. However, some recent results with Preisach models (Ktena *et al.*, 2001 and 2002) have shown discrepancies attributed to the choice of hysteresis operators.

Additionally, sometimes the wiping-out and congruency properties (Mayergoyz, 1991) required for the application of the Preisach formalism are not observed in the ε - T SMA hysteresis and this model cannot be used (Nascimento, 2002).

In this paper, it is proposed an adaptation of the Limiting Loop Proximity (L^2P) hysteresis model, recently developed by Almeida *et al.* (2002) for magnetic hysteresis and later adapted to thermal hysteresis in VO_2 thin films (Almeida *et al.,* 2002), to describe hysteretic ε - T characteristics of a SMA actuator. All parameters necessary for the modeling procedure was determined using an experimental set-up especially designed for this study.

2. Modelling the ε - T hysteretic behavior

Figure (1) shown a schematic representation of typical hysteresis in ε - T characteristics of a SMA wire actuator. Hysteresis trajectories corresponding to low temperatures excursions are usually confined inside the major limiting loop, which is the combination of the descending and ascending limiting curves. Based on the models developed by Almeida *et al*. (2002), the following function $F_L(T)$ for the $\varepsilon(T)$ behavior is proposed

$$\varepsilon(T) = F_L(T) = \frac{\varepsilon_s}{\pi}\left[\arctan\left(\beta\left(\delta\frac{w}{2} + T_c - T\right)\right) + \frac{\pi}{2}\right] + \varepsilon_0 \tag{1}$$

to describe the strain ε pertaining to the major descending and ascending limiting curves. In this equation T is the excitation temperature, ε_0 is the saturation strain, ε_s is the hysteresis height, w is the hysteresis width, β is related with $\frac{d\varepsilon}{dT}$ at T_c, where T_c is the critical temperature at the center of the hysteresis curve. δ is an operator defined as $\delta = \mathrm{sgn}\left(\dot{T}\right)$. The combination of the curves $F_L(T, \delta = +1)$ and $F_L(T, \delta = -1)$ describes the major hysteresis loop in the ε - T plane.

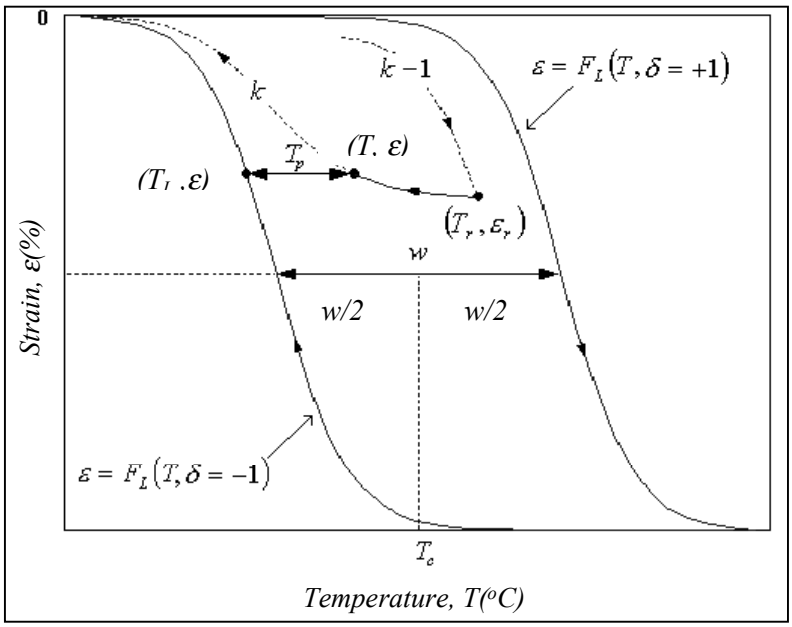

Figure 1. Schematic representation of hysteresis in ε - T characteristics of a SMA wire actuator. This geometric construction of a reversal curves illustrates the concept of proximity of a point on the reversal curve to the limiting loop.

Reversal curves, minor loops and nested minor loops are not described by Eq. (1). This equation must to be modified to represent the dependence $\varepsilon(T)$ for any trajectory inside the limiting major loop. To introduce this modification, it is particularly important to take into account the way in which the inner trajectories approach the major loop. This concept is illustrated in Fig. (1), where the change in the sign of dT/dt that occurs in at the time instant t_r is represented (point (T_r, ε_r)). Hysteresis branch *k-1* is reversed, and *k* starts at the reversal point (T_r, ε_r).

The *proximity temperature* T_p in Fig. (1) is introduced to express the nearness in distance of the current point (T, ε) on branch *k* to the corresponding point (T_L, ε) on the limiting curve $F_L(T, \delta)$, given as

$$T_p = T_L - T \tag{2}$$

Using Eq. (1) to obtain the value of T_L corresponding to $\varepsilon = F_L(T_L\ ,\ \delta)$

$$T_L = \delta\frac{w}{2} + T_c - \frac{1}{\beta}\left(\tan\pi\left(\frac{\varepsilon-\varepsilon_0}{\varepsilon_S}\right) - \frac{\pi}{2}\right) \tag{3}$$

Thus, T_p at $(T,\ \varepsilon)$ as obtained from Eq. (2) is

$$T_p = \delta\frac{w}{2} + T_c - \frac{1}{\beta}\left(\tan\pi\left(\frac{\varepsilon-\varepsilon_0}{\varepsilon_S}\right) - \frac{\pi}{2}\right) - T \tag{4}$$

In the beginning of a new trajectory at the reversal point $(T_r,\ \varepsilon_r)$, the proximity function T_p is named T_{pr}, calculated as follow:

$$T_{pr} = \delta\frac{w}{2} + T_c - \frac{1}{\beta}\left(\tan\pi\left(\frac{\varepsilon-\varepsilon_r}{\varepsilon_S}\right) - \frac{\pi}{2}\right) - T_r \tag{5}$$

It was observed from experimental data that T_p exhibits almost the same functional dependence regardless of the reversal point $(T_r,\ \varepsilon_r)$ at which the reversal curve starts. Thus, to describe T_p for any branch inside the major loop, the following functional dependence is proposed :

$$T_P = T_{pr}P(x) \tag{6}$$

where

$$x = \left(\frac{T-T_r}{T_{pr}}\right) \tag{7}$$

and $P(x)$ is an arbitrary monotonically decreasing function, with P(0) = 1 and P(∞) = 0, called here the *proximity function*. Thus, for a hysteresis branch reversed at the point $(T_r,\ \varepsilon_r)$ inside the major ε - T loop, the strain for any arbitrary point (T,ε) is expressed as

$$\varepsilon(T) = \frac{\varepsilon_s}{\pi}\left[\arctan\left(\beta\left(\delta\frac{w}{2} + T_c - T - T_{pr}P(x)\right)\right) + \frac{\pi}{2}\right] + \varepsilon_0 \tag{8}$$

and the values of δ, T_r and T_{pr} changes only at the reversal points, and remain unchanged until the next reversal in dT/dt occurs. For the SMA actuator employed in this study, the following proximity function is proposed

$$P(x) = -\frac{x}{2} - \frac{1}{4a}\ln\left(\left|\tanh^2 a(x-b) - 1\right|\right) - c \tag{9}$$

where a and b are arbitrary constants and c is chosen such that $P(\infty) = 0$.

3. Experimental procedure

3.1. Experimental set-up

The SMA actuators used in this work are equiatomic Ni-Ti wires with 90mm in length and 150μm in diameter, supplied by Mondo-Tronics Inc. (Gilbertson, 2000). In order to determine the ε - T characteristic of the Ni-Ti SMA wire, an experimental platform illustrated in Fig. (2) was implemented to submit the SMA wire to several heating-cooling cycles. As shown in Fig. (2), the experimental set-up has three fundamental parts: a simple mechanical structure, a voltage/current converter and a data acquisition system. In the mechanical structure of the test bench, the SMA wire (8) is loaded with a constant weight (5) and electrically heated by a voltage/current converter. A linear differential transformer (LVDT (1)) having a resolution of 5μm is used to measure the displacement of the SMA wire. External room temperature disturbances are greatly reduced by embedding the wire in a heat-insulating medium. Figure (3) shows a picture of this experimental test bench.

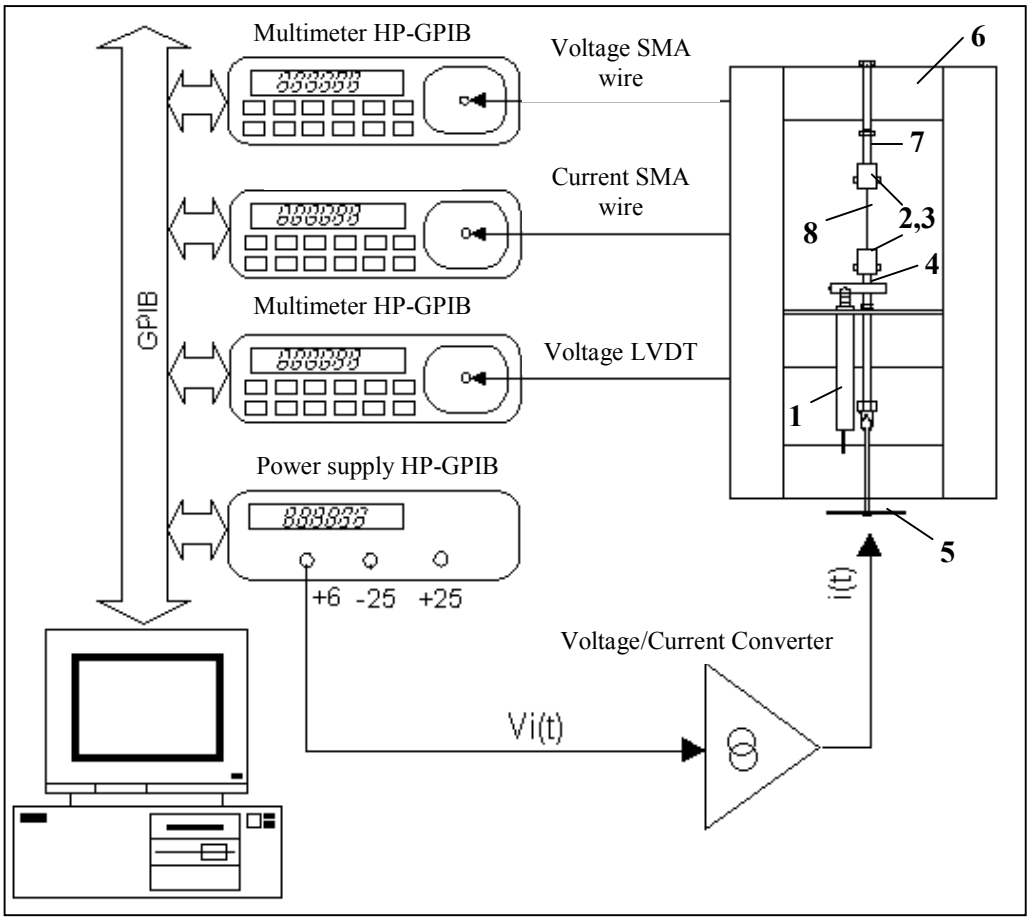

Figure 2. Mechanical structure of the testing bench and data acquisition system: (1) LVDT displacement sensor; (2), (3) mechanical grips; (4) guiding LVDT; (5) load (weight); (6) frame; (7) guiding rod; (8) SMA wire.

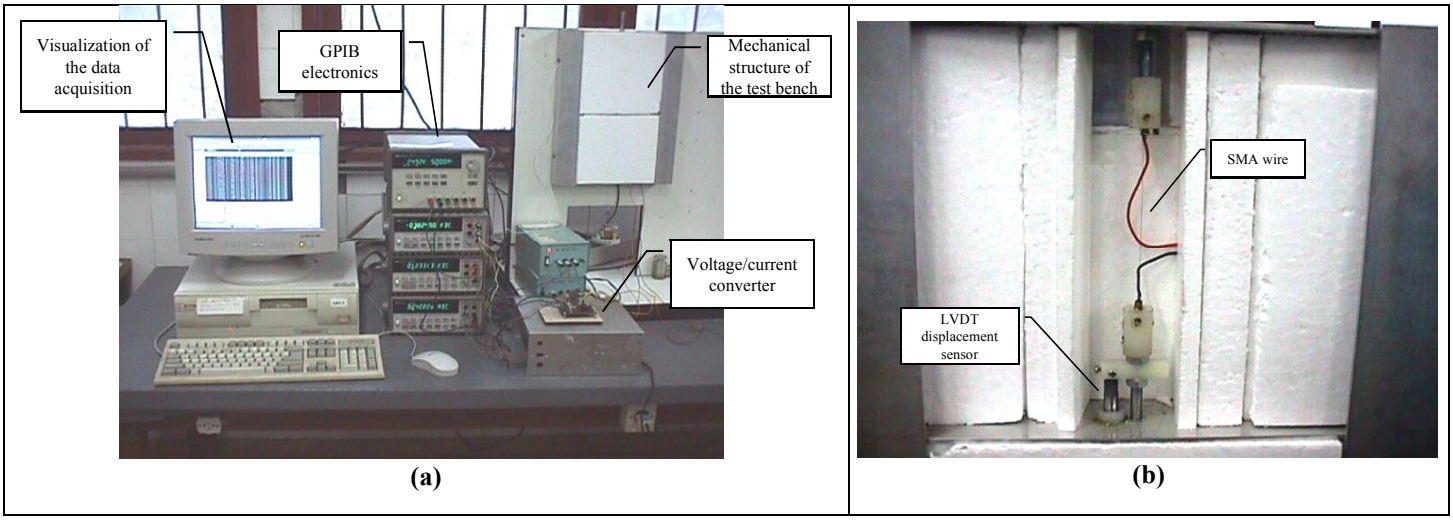

Figure 3. Picture of the test apparatus. (a) Entire view. (b) Zoom view of the SMA wire actuator.

In the absence of an accurate and reliable technique for direct measurement of the SMA wire temperature it was estimated from the heat-transfer thermal equilibrium equation given by

$$\rho c_p V \frac{dT}{dt} = Ri^2 - hA(T - T_\infty) \tag{10}$$

where V, A and R are the volume, the surface area and the electrical resistance of the SMA wire, respectively. The specific mass ρ and the specific heat c_p are intrinsic properties of the material and h is the convective heat transfer coefficient between the wire and its surroundings at temperature T_∞. The steady-state value of the wire temperature, for a step current I when $dT/dt = 0$ is

$$T_{ss} = \frac{R}{hA} I^2 + T_\infty \tag{11}$$

The control of the heating electrical current I through the wire and measurement of the steady-state wire deformation with an LVDT (1), was done using GPIB compatible instruments, as illustrated in Fig. (2).

3.2. Estimation of the convective heat transfer coefficient (h)

In some studies concerning simulation of electrical heating of SMA wires, the convective heat transfer coefficient (h) has been chosen from the literature. However, this is not an easy task, as demonstrated by the results of Brailovski *et al.* (1996). Additionally, Reynaerts and Van Brussel (1998) present a data collection for h which confirm the difficulty to choice this parameter. Thus, an identification procedure was employed to determine the h value to be used in Eq. (11). Considering that R and I are for the steady state in Eq. (10), the following identification problem is established

$$R_n I_n^2 = hA(T_n - T_\infty); \; n = 1, 2, \ldots, N \tag{12}$$

where N is the number of samples. For application of the parameter estimation process, R_n and T_n were determined experimentally with the TiNi wire maintained in an electrical furnace. These values were compared with R_n and I_n measured from the experimental platform showed in Fig. (3). Using the identification method proposed by Ljung (1999), Eq. (12) can be rewritten as

$$y(x) = BT(x) - C \tag{13}$$

with $B = hA$, $C = hAT_\infty$ and $y(x) = R_n I_n^2$.

By applying the least squares method for the Eq. (13), the following values were identified: h = 88,2 W/m^2.^{o}C and T_∞ = 25,1^{o}C.

4. Results and discussions

To obtain the model parameters, the SMA wire was submitted to a time-varying current excitation, composed of various monotonic segments. The wire temperatures, for a current rate of 4,78 *mA/min* used in all experiments, was estimated by Eq. (11), as can be verified in Fig. (4) for major and minor loops.

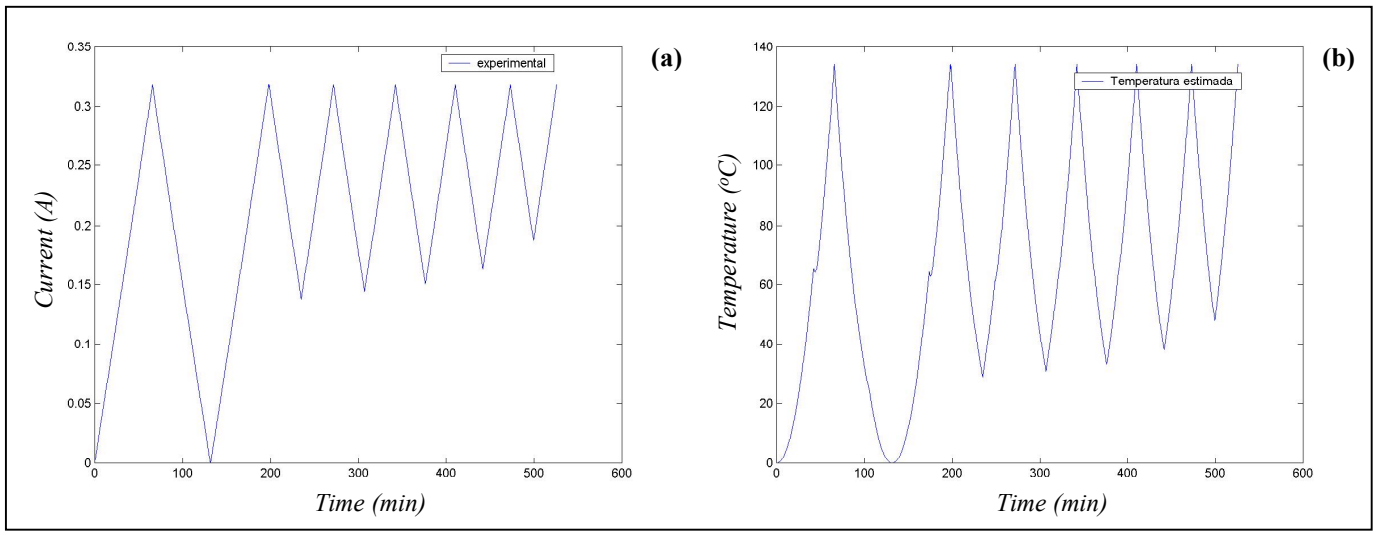

Figure 4. Current and temperature waveforms on the SMA wire actuator. (a) Excitation wire current. (b) Estimated wire temperature.

Figure (5) shows the strain response of the SMA actuator for the major loop excitation verified in Fig. (4). The experiments were carried out for various applied load (weights) between 2,5 and 4 *N* corresponding to uniaxial tensile stresses between 142 and 225 *MPa*.

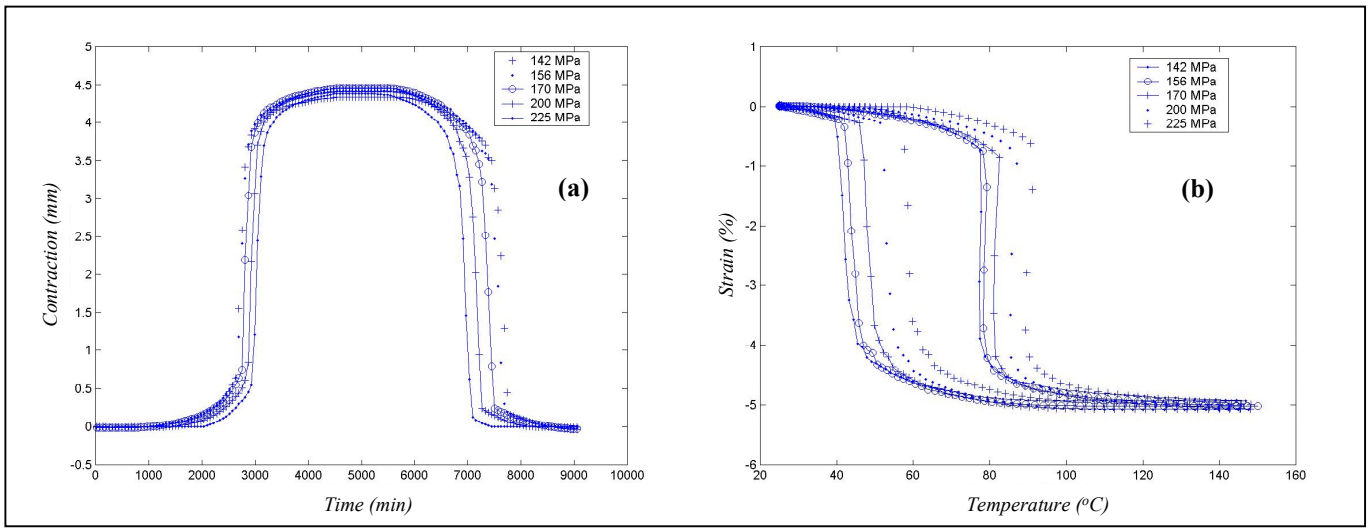

Figure 5. SME behavior of the actuator wire for several applied loads. (a) Absolute contraction of the SMA wire. (b) ε - T loops.

It is observed from Fig. (5) the displacement of the ε - T loops towards the higher temperatures. This behavior is typical of the SMA actuators and corresponds to an increase of the transformation temperatures with the applied stress, according to a modified Clausius-Clayperon law (Otsuka and Wayman, 1998). The calculated stress/temperature rate was of the order of 6,8 *MPa/°C* and 4,4 *MPa/°C* for austenite and martensite temperatures, respectively. The same value of saturation strain (~5%) for various stress levels in Fig. (5b) is due to the fact that between 142 and 225 *MPa* the martensite variants into the SMA wire are fully oriented by the external load.

From inspection of the ε - T loops shown in Fig. (5b), the values of ε_0, ε_s, w and T_c can be readily determined for any applied stress. However, it is not possible to determine β, a and b from inspection of experimentally obtained curves. The value

of β can be obtained by fitting both $F_L(T, \delta = +1)$ and $F_L(T, \delta = -1)$ to experimental major descending and ascending curves, respectively. Once the values of ε_0, ε_s, w, T_c and β have been determined, the value of a and b in $P(x)$ can be obtained by fitting Eq. (8) to a first-order descending ε - T curve. A first-order descending curve is generated by first increasing the current to maximum value, and then reducing the temperature monotonically until it reaches some value I such that the strain ε lies on the ascending major curve. Subsequently, the current is again increased monotonically to maximum value.

For the SMA wire employed in this study, the values obtained for the five parameters are: ε_s = 4,8%, ε_0 = -4,6%, β = 0,3°C^{-1}, T_c = 71,5°C, a = 5 and b = 1,028. For the estimated temperature using Eq. (11), the parameters are: h = 88 W/m^2.°C, A = 3,68x10^{-5} m^2 and the value of R is the one measured during the experiments (Nascimento, 2002). Additionally, it was experimentally verified that hysteresis width (w) is a linear function of the applied stress (σ). From the w results obtained on Fig. (5b), it was confirmed the following relationship between w and σ:

$$w(\sigma) = -0{,}0764\sigma + 47{,}9492 \tag{12}$$

Figure (6) presents the experimental ε - T curves (solid symbols) for 200MPa together with the respective simulated behavior (solid line) for a major loop and minor loops calculated from Eq. (8) incorporating Eq. (12). These results were obtained with the excitation waveforms described in Fig. (4).

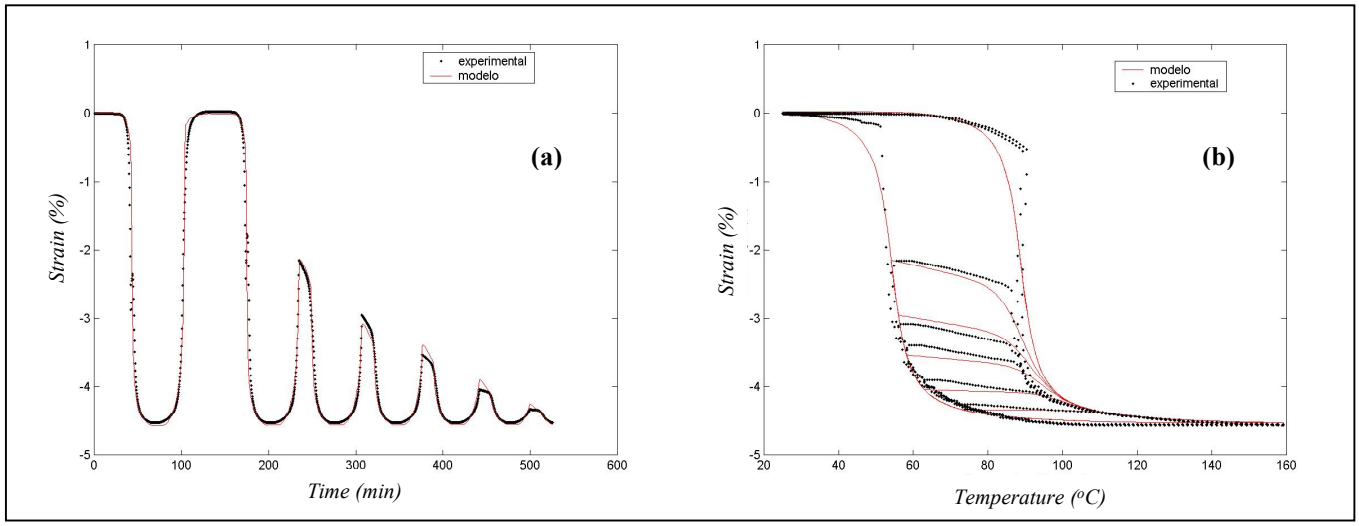

Figure 6. Response of the SMA wire actuator under 200MPa. (a) SMA strain response as a function of the time. (b) experimental and simulated major and minor loops for the SMA wire actuator.

From Fig. (6a) and Fig. (6b) it is verified a good agreement of the data calculated with the proposed model and experimental data. To quantify the discrepancy between model and experimental data, the normalized root-mean-square error was employed, given as

$$e_{RMS} = \sqrt{\frac{\sum_{i=1}^{N}(x_i - \bar{x}_i)^2}{\sum_{i=1}^{N}\bar{x}_i^2}} x100\% \tag{13}$$

where x_i represents data from the model, $\bar{x}_i$ represents experimental data and N is the number of data points. Using N = 1594, the mean error for all first-order descending ε - T curves was calculated to be 5,4%.

5. Conclusions

In this work a phenomenological model for the SMA actuator ε - T behavior has been proposed and successfully implemented. This model was established directly from the Limiting Loop Proximity (L^2P) hysteresis approach, originally developed for magnetic hysteresis and later adapted to describe thermal hysterisis in VO_2 thin films. This model is expressed in the form of an algebraic equation that is computationally simple to implement. The parameters of this model were determined experimentally from experimental data with regard to major and minor ε - T loops. Aiming a more correct result, the convective heat transfer coefficient for temperature estimation was determined by an identification parameter procedure. The obtained

results can be considered satisfactory. The discrepancies between the calculated and the experimental data can be attributed to limitations in the numerical implementation of the model and to the large asymmetry of ε - T curve. The model has potential to be applied for control purposes in smart structures.

6. Acknowledgments

The authors thank CNPq/PRONEX (Conselho Nacional de Desenvolvimento Científico e Tecnológico) and CAPES (Fundação de Coordenação de Aperfeiçoamento de Pessoal de Nível Superior) for the award of research and study fellowship during the course of these investigations.

7. References

Almeida, L. A. L., Deep, G. S., Lima, A. M. N. and Neff, H., 2002. "The Limiting Loop Proximity (L^2P) Hysteresis Model", IEEE Transaction on Magnetics, Vol. 39(1), pp. 523-528.

Almeida, L. A. L., Deep, G. S., Lima, A. M. N. and Neff, H., 2002. "Modeling of the Hysteretic Metal-Insulator Transition in Vanadium Dioxide Infrared Detector", Optical Engineering, Vol. 41(10), pp. 2582-2588.

Auricchio, F. and Lubliner, J., 1997. "A Uniaxial Model for Shape Memory Alloys", International Journal of Solids and Structures, Vol.34, n.27, pp. 3601-3618.

Auricchio, F. and Sacco E., 1997. "A One-Dimensional Model for Superelastic Shape Memory Alloys with Different Elastic properties Between Austenite and Martensite", International Journal of Non-Linear Mechanics, Vol. 32, n.6, pp.1101-1114

Auricchio, F., Taylor, R.L. and Lubliner, J., 1997. "Shape-Memory Alloys: Macromodeling and Numerical Simulations of the Superelastic Behavior", Comp. Methods in Applied Mech. and Eng., Vol.146, pp. 281-312.

Boyd, J.G. and Lagoudas, D.C., 1994. "Constitutive Model for Simultaneous Transformation and Reorientation in Shape Memory Alloys", Mech. of Phase Transf. and Shape Memory Alloys, L.C. Brinson and B. Moran (Eds), ASME New York, pp. 159-177.

Brailovski, V., Trochu, F. and Daigneault, G., 1996. "Temporal characteristics of shape memory linear actuators and their application to circuit breakers", Materials and Design, Vol. 17, N^o 3, pp. 151-158.

Brinson, L.C., 1993. "One Dimensional Constitutive Behavior of Shape Memory Alloys: Themomechanical Derivation with Non Constant Material Functions and Redefined Martensite Internal Variable", Journal of Intelligent Materials Systems and Structures, n.4, Vol.2, pp. 229-242.

Gilbertson, R. B., 2000. "Muscle Wires Projet Book", Mondo-Tronics Inc., 55p.

Gorbet, R. B., 1997. "Control of Hysteretic Systems with Preisach Representations". PhD Thesis: University of Waterloo, Waterloo, Canada, 176p.

Helm, D. and Haupt, P., 2003. "Shape memory behaviour: modelling within continuum thermomechanics", International Journal of Solids and Structures, Vol. 40, pp. 827–849.

Ktena, A., Fotiadis, D.I., Spanos, P.D. and Massalas, C.V., 2001. "A Preisach model identification procedure and simulation of hysteresis in ferromagnets and shape-memory alloys", Physica B, Vol. 306, pp. 84–90.

Ktena, A., Fotiadis, D.I., Spanos, P.D., Berger, A. and Massalas, C.V., 2002. "Identification of 1D and 2D Preisach models for ferromagnets and shape memory alloys", International Journal of Engineering Science, Vol. 40, pp. 2235–2247 (article in press).

Liang, C. and Rogers, C.A., 1990. "One-Dimensional Thermomechanical Constitutive Relations for Shape Memory Materials", Journal of Intelligent Materials Systems and Structures, n. 1, Vol.2, pp. 207-234.

Ljung, L., 1999. "System Identification: Theory for the User", Prentice Hall, Linkoping University, Sweden.

Majima, S., Kodama, K. and Hasegawa, T., 2001. "Modelling of Shape Memory Alloy Actuator and Tracking Control Systems with the Model", IEEE Transactions on Control Systems Technology, Vol.9, pp. 54-59.

Mayergoyz, I., 1991. "Mathematical Models for Hysteresis", Springer-Verlag, 273p.

Nascimento, M.M.S.F., 2002. "Contribution to the Study of Hysteresis in Shape Memory Alloys" (in Portuguese). Master of Science Report: Universidade Federal de Campina Grande, Brazil, 79p.

Ortin, J. and Delaey, L., 2002. "Hysteresis in shape-memory alloys", International Journal of Non-Linear Mechanics, Vol. 37 pp. 1275 – 1281.

Otsuka, K. and Wayman, C.M., 1998. "Shape Memory Materials", Cambridge University Press, Cambridge, UK, 284p.

Paiva, A. and Savi, M. A., 1999. "On The Constitutive Models With Assumed Transformation Kinetics For Shape Memory Alloys" (in protuguese), Proceedings of the 15th Brazilian Congress of Mechanical Engineering, CD-ROM, Águas de Lindóia-SP, Brazil.

Reynaerts, D. and Van Brussel, H., 1998. "Design Aspects of Shape Memory Actuators", Mechatronics, Vol. 8, pp. 635-656.

Srinivasan, A.V. and McFarland, D.M., 2001. "Smart Structures – Analysis and Design", Cambridge University Press, Cambridge, UK, 228p.

Tanaka, K. and Nagaki, S., 1982. "Thermomechanical Description of Materials with Internal Variables in the Process of Phase Transformation", Ingenieur – Archiv., Vol.51, pp.287-299.

Tanaka, K., 1986. "A Thermomechanical Sketch of Shape Memory Effect: One – Dimensional Tensile Behavior", Res. Mech., Vol. 18, pp. 251.